Science of the Total Environment 876 (2023) 162810

Contents lists available at ScienceDirect

Science of the Total Environment

journal homepage: www.elsevier.com/locate/scitotenv

Misinterpretation in microplastic detection in biological tissues: When 2D imaging is not enough

Alba Benito-Kaesbach [a], Jose Manuel Amigo [b,d], Urtzi Izagirre [a], Nerea Garcia-Velasco [a], Laura Arévalo [c], Andreas Seifert [b,c], Kepa Castro [d,*]

[a] Cell Biology in Environmental Toxicology (CBET) Research Group, Dept. Zoology and Animal Cell Biology, Faculty of Science and Technology and Research Centre for Experimental Marine Biology and Biotechnology PIE-UPV/EHU, University of the Basque Country UPV/EHU, E-48080 Bilbao, Basque Country, Spain
[b] IKERBASQUE, Basque Foundation for Science, Euskadi Plaza 5, 48009 Bilbao, Spain
[c] CIC nanoGUNE BRTA, Tolosa Hiribidea 76, 20018 San Sebastian, Spain
[d] IBeA Research Group, Analytical Chemistry Department, Faculty of Science and Technology, University of the Basque Country UPV/EHU, E-48080 Bilbao, Basque Country, Spain

HIGHLIGHTS

- We detected 1 μm polystyrene particles by Raman imaging in cryosections of mussels.
- We detected the microplastics in the epithelium by 2D Raman imaging analysis.
- 3D Raman imaging showed microplastics moved there during sample preparation.
- Spectroscopists have to be aware about possible imaging data misinterpretation.
- Data misinterpretation can also happen when samples are fortuitously contaminated.

GRAPHICAL ABSTRACT

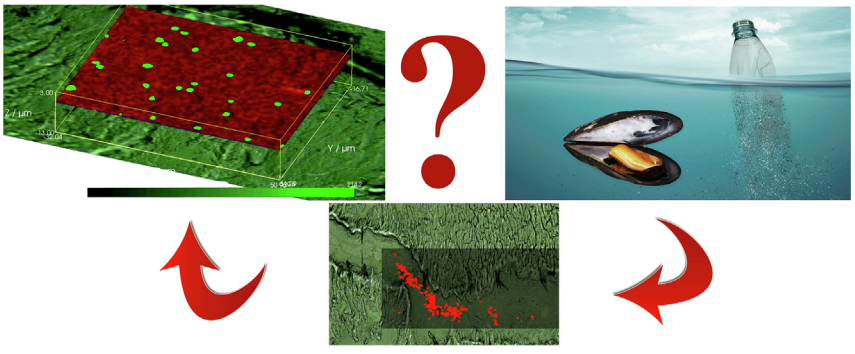

ARTICLE INFO

Editor: Damià Barceló

Keywords:
Microplastics
Raman imaging
Mussels
Polystyrene
Cryotome

ABSTRACT

The presence of microplastics in the food chain is a public concern worldwide, and its analysis is an analytical challenge. In our research, we apply Raman imaging to study the presence of 1 μm polystyrene microplastics in cryosections of *Mytilus galloprovincialis* due to its wide geographic distribution, widespread occurrence in the food web, and general high presence in the environment. Ingested microplastics are accumulated in the digestive tract, but a large number can also be rapidly eliminated. Some authors state that the translocation of microplastics to the epithelial cells is possible, increasing the risk of microplastics transmission along the food chain. However, as seen in our study, a surface imaging approach (2D) is probably not enough to confirm the internalization of particles and avoid misinterpretation. In fact, while some microplastic particles were detected in the epithelium by 2D Raman imaging, further 3D Raman imaging analysis demonstrated that those particles were dragged from the lumens to the epithelium during sample preparation due to the blade drag effect of the cryotome, and subsequently located on the surface of the analyzed cryosection, discarding the translocation to the epithelial cells. This effect can also happen when the samples are fortuitously contaminated during sample preparation. Several research articles that use similar analytical techniques have shown the presence of microplastics in different types of tissue. It is not our intention to put such results in doubt, but the present work points out the necessity of appropriate three-dimensional analytical methods including data interpretation and the need to go a step further than just surface imaging analysis.

* Corresponding author.
E-mail address: kepa.castro@ehu.eus (K. Castro).

http://dx.doi.org/10.1016/j.scitotenv.2023.162810
Received 24 January 2023; Received in revised form 6 March 2023; Accepted 8 March 2023
Available online 13 March 2023

1. Introduction

Regardless of its unlimited range of applications and its pivotal role in the development of modern society, plastic has become an environmental threat. For example, big parts of the produced polystyrene (PS), the 6th most demanded plastic in Europe in 2018 (De-la-Torre et al., 2020), unfortunately ends up in the marine environment (Erni-Cassola et al., 2017).

Public concern for the potential adverse effects of plastics (Fang et al., 2020) has been focused on the so-called microplastics (MPs), a group of plastic debris in the range of 1 μm to 5 mm (Jin-Feng et al., 2018; Mendoza et al., 2018). Regardless of how MPs are generated they are bioavailable to a wide range of invertebrates (Browne et al., 2008), especially to low trophic filter feeders, detritivores and planktivorous (Wright et al., 2013), because they occupy the same size fraction as sediments and planktonic organisms. Therefore, they may accumulate within organisms by direct ingestion (Xu et al., 2019) or trophic transfer (Li et al., 2019), producing physical harm through internal abrasions and blockages.

Ingested MPs are accumulated in the digestive tract of mussels in a short time. However, a large number of them can also be rapidly eliminated (Calmão et al., 2023). Hence, it is important to determine the capacity of plastics to be incorporated into the cells to assess the consequential damages. It is proven that cells with phagocytic activity, such as mussel hemocyte, can internalize MPs (Katsumiti et al., 2021; Von Moos et al., 2012). Nevertheless, cells used in these studies are cultured cells out of the protection of the lining epithelium and tissue barriers. Thus, it needs more studies based on histological and imaging approaches to observe the microplastic internalization into cells and tissues.

Sampling and analyses of MPs become more difficult and demanding the smaller the particles are, which is one reason why most of the MP surveys analyze only a size range from 0.3 to 5 mm, a range where visual sorting is an appropriate approach (Lenz et al., 2015). Nevertheless, organisms such as filter feeders capture and retain 3–4 μm particles with 100 % efficiency and can ingest particles as small as 1 μm diameter (with a reduced efficiency of 50 %) (Wright et al., 2013). Since small particles (< 100 μm) are the most harmful (Primpke et al., 2020) and present ones in the highest concentrations (Enders et al., 2015), more research regarding these sizes is required.

To manage and control this emerging pollutant, standardized methods for isolation, detection and identification of MPs are needed for particles as small as 1 μm (Noventa et al., 2021; Shim et al., 2017), which are the target of this study.

Various methods have been applied to isolate MPs in biological tissues (Yu et al., 2019), particularly highlighting the chemical digestion method (Zhu and Wang, 2020). However, such techniques do not allow studying the spatial distribution of MPs ingested by the organism, which is key from a toxicological point of view. It is important to know whether these MPs accumulate in the mussel through ingestion rather than through adherence to the surface of the tissue (Kolandhasamy et al., 2018).

In contrast, cryosection technique is very useful for investigating the translocation of MPs to other tissues and could serve for investigating the exact position of the particles ingested by living organisms (Collard et al., 2017). Irazola et al. (Irazola et al., 2015) used cryosection and paraffin-embedded sections to study the accumulation and distribution of MPs in different tissues of mussels *Mytilus galloprovincialis,* concluding that frozen tissue allows for better detection of MPs than paraffin-embedded tissue. In fact, MPs were dissolved during the sample preparation in paraffin, as organic solvents are usually used.

Regarding the detection and identification step, there are many analytical tools (Xu et al., 2019). However, the most common techniques used to analyze MPs in biological samples are Fourier-transform infrared (FTIR) and Raman spectroscopy (Käppler et al., 2016), which require small sample amounts, are applicable with high accuracy, and allow even for the determination of particle size distributions (Araujo et al., 2018; Elert et al., 2017).

As the diameter of the laser beam is smaller in Raman spectroscopy, this method allows for the identification of particles of smaller size down to 1 μm (Araujo et al., 2018; Nguyen et al., 2019; Xu et al., 2019). However, scarce studies have reported the identification of 1 μm MPs, mainly because their identification depends also on other parameters such as the complexity of the sample (difficult isolation), applied filter type, and measurement parameters (Nguyen et al., 2019; Xu et al., 2019), among others.

Despite the typical Raman point analysis, which has been extensively applied to study MPs in biological samples of marine organisms (Dehaut et al., 2016; Li et al., 2019), chemical imaging for this purpose has begun quite recently. For example, Leung et al. (2021) used an automated mapping approach to detect 5 different types of plastics in digested samples of *Perna viridis,* detecting particles in a size range of 30–820 μm.

Chemical imaging techniques are accepted as promising tools for MPs analysis in surfaces (Fang et al., 2020; Xu et al., 2019), particularly when structured samples, such as direct analysis of tissues, are under study. Therefore, when a biological matrix (such as cryosection) is mapped by Raman spectroscopy, it might be possible to specifically identify where the MPs are accumulated inside the mussel, to determine the relative amount, and even the size of the particles. However, as Elert et al., 2017 investigated, the spectroscopic scanning methods are clearly more time-consuming than the extraction methods. For example, Imhof et al., 2016 and Vianello et al., 2013 reported that only ≈ 2 % or ≈ 5 % of the sample could be analyzed in Raman imaging, respectively.

Nevertheless, one of the advantages of spectroscopic techniques, as for example Raman imaging, is the analysis of particle size distribution by visual image, a feature that can only be studied with high-resolution microscopy techniques (Elert et al., 2017). In comparison to Raman imaging, FTIR imaging leads to significant underestimation (about 35 %) of MPs, especially in the size range lower than 20 μm. Unfortunately, the measurement time of Raman imaging is quite long compared to FTIR imaging (Käppler et al., 2016).

In a nutshell, one method alone will not fulfil all the requirements to provide a comprehensive dataset for wide-ranging detection of MPs. Raman imaging yields more detailed information about the chemistry of the particles and their size and distribution. However, it presents disadvantages such as the limited sample surface that can be investigated in a single run in a reasonable time and frequent difficulties with contamination of the organic matrix in the sample, which could be considered as important drawbacks to applying this method for fast evaluation of MPs in the environment.

In general, chemical imaging analysis (such as Raman or FTIR imaging analysis) has been understood as the identification of specific molecules on a surface (2D imaging analysis). That way, microplastics analysis has been carried out, too, as in Levermore et al., 2020. As presented in this research work, the current technical capabilities of modern instrumentation allow for volumetric chemical analysis (3D imaging analysis) thanks to the high confocality of modern microscopes (Mattson et al., 2013), which opens up new interesting analytical approaches for studying microplastics (Tarafdar et al., 2022). Interesting research articles employing 3D Raman imaging to analyze cells can be found in literature (Kallepitis et al., 2017; Lin et al., 2020; Wei et al., 2019). However, only a few studies use this technique for microplastics analysis, for example, Chen et al., 2017, who study polystyrene beads of 10 and 100 μm diameter in 3D volumes and lipid droplets in adipose cells.

In our research, we study the capability of Raman imaging as a useful technique to study the presence and distribution of 1 μm polystyrene MPs in cryosections of biological matrices. By virtue of its wide geographic distribution, sessile lifestyle, basal position on the food web, easy sampling, its well-understood biology, and high accumulation of a wide range of pollutants (including MPs), *M. galloprovincialis* was chosen as the model organism in our study. Moreover, it represents an animal for human consumption, which adds value to its use in this type of study. The proposed approach identifies the distribution of particles inside the organism, particularly in the digestive gland as the target organ in this work. We will point out possible data misinterpretation based on 2D (surface) imaging, and highlight the benefits of 3D (volume) imaging.

2. Experimental section

2.1. Microplastic standards and mussel samples

As polystyrene is one of the most used plastics, one of the most present in marine environments, and it degrades quite easily and generates microplastics to a high extent, commercial fluorescent microspheres of polystyrene (PS) with a size of 1 μm were used to carry out the experiment (Fluoro-Max™ Green Fluorescent Polymer Microspheres, Thermo Fisher Scientific, catalogue number G0100). The MP solution had a concentration of 1 % (*w*/w) of fluorescent microspheres and a density of 1.05 g/cm^3. To avoid misinterpretation due to cross-contamination of the biological tissues with microplastics from the environment (laboratory, clothes, water, etc.), we used labeled particles, fluorescent particles in this case.

Mytilus galloprovincialis (4.82 ± 0.8 cm -maximum distance between the umbo and the posterior margin of the shell; 1.56 ± 0.5 g-biomass, mean ± SD) were collected from the estuary of Butron river, in Plentzia, Bizkaia, 43°24′33.6"N 2°56′51.5"W, on the 14th of March 2021. Mussels were collected from the rocks when the tide was low by carefully cutting byssal threads to avoid damaging the underlying soft tissues. 15 mussels were collected, which were subsequently washed with seawater to remove the remains of sand and organic matter. Once cleaned, they were left in a tank full of seawater with constant water renewal to carry out their depuration in the Plentzia Marine Station, University of the Basque Country (PiE-UPV/EHU) for at least 48 h to allow elimination of the gut contents before analysis of the soft tissues (Soto et al., 1995).

2.2. Setup for sample preparation

Exposures to PS MPs were performed in food absence, persistent aeration, a constant temperature of 16 °C and a 12/12 h light/dark regime. Two glass beakers (300 mL) were filled with 250 mL of seawater previously filtered with a 0.2 μm filter. In each glass beaker 3 mussels were introduced, one beaker serving as control, the other for exposure to PS with 5.5 × 10^6 particles/mL.

We used an MP concentration much higher than those recorded in marine environments to ensure that the mussels retain plastics. The higher the concentration, the more certain one can be to find the particles. Applicable doses in laboratory tests have been discussed (Lenz et al., 2016) and criticised in research works focused on uptake ratios, MP total mass calculations in animals, epidemiologic/incidence/toxicological studies, etc. However, this is not the purpose of our research work here. The conclusions of our study do not focus on the amount of microplastics present in the tissues, or on the rate of translocation into the tissues, but rather on whether or not they are inside the tissue, and whether our analytical approach allows us to detect them including spatial information.

The mussels were exposed to the particles for 24 h, which is long enough for them to filter MPs in the water column. Mussels were maintained with constant intense aeration to maximize buoyancy and ensure that the MPs stayed in the water column for as long as possible. The mussels were collected after the exposure to MPs, and their shells were washed with distilled water to prevent contamination and remove MPs adsorbed on the shell surfaces. Later, the shell was removed, and the inner soft tissue was carefully isolated and prepared for cryosection. All glassware and instruments were washed with distilled water to prevent contamination.

The location of the MPs in mussel tissues was studied using cryosectioning. A cross-section of the soft tissue was frozen with liquid nitrogen. For this purpose, the sample was placed on a floating metallic plate to ensure slow freezing and avoid crystallization. The sample was positioned such that a complete cross-section of the mussel could be prepared. Once the soft tissues were frozen, they were stored in a metallic plate in a freezer at −40 °C until use. Tissue sections were prepared with a Leica CM 3050S Cryostat equipped with a motorized cutting device at a chamber temperature of −25 °C. The cross-sections of the mussels were fixed to a metallic chuck by adding a cryo-embedding medium. The cryosections of 10 μm thickness were collected onto glass slides and kept at room temperature, causing tissue sections to flash-dry immediately upon contact. Two or three tissue sections were collected onto every glass slide. All the cryosections were quickly screened under the Leica Microscope. Sections with the best conditions and the greatest proportion of the digestive gland were chosen to search the MPs and to study the distribution of the particles in the lumen and epithelium of the digestive tract.

During sectioning, all blades and anti-rolls were changed after each treatment, and all materials in direct contact with the samples were cleaned with acetone to avoid cross-contamination by MPs. Blanks were used to verify that the cleaning of the cryotome was effective. The blanks were mussels free of fluorescent MPs (not fed with fluorescent MPs). Cryosections of these mussels were analyzed under a fluorescence microscope to verify that no MPs were present, that is, no MP contamination was produced in the cryotome.

2.3. Setup for Raman spectroscopy and imaging

A Renishaw inVia confocal Raman microscope (Renishaw, Gloucestershire, UK), was used for Raman point-by-point and imaging analysis. The measurements were carried out with a 532 nm excitation laser (Renishaw, Gloucestershire, UK, RL532C50) with a nominal out-put power of 300 mW. The system has a CCD detector cooled by Peltier effect (−70 °C), and it is coupled to a Leica DMLM microscope (Bradford, UK) that allows the microscopic analysis of the sample by using 5× N PLAN (0.12 NA), N PLAN EPI (0.40 NA), and 50× N PLAN (0.75 NA) and 100× (LMPlanFL N 0.80 NA) objectives. The nominal power of the source goes from 0.05 % to 100 % of the total power. To avoid thermal decomposition of the sample, the nominal power of the laser was adjusted.

For Raman image mapping, the samples were scanned using a 50× objective lens (theoretical laser spot size diameter on the focal plane at 532 nm is 0.87 μm), with an integration time of 3.5–5 s and a spatial resolution of 1 μm/pixel in all axes (XYZ), at an operating spectral resolution smaller than 1 cm^{-1}. To generate the image, the net intensity of the main characteristic peak of polystyrene MPs at 1001 cm^{-1} (see supplementary material Fig. S1) was plotted in the mapped area. Baseline correction, smoothing and cosmic ray removal of the acquired spectra were performed with the Renishaw WiRE 4.2 software, as well as to obtain the Raman images. The InVia spectrometer was calibrated daily, setting the 520.5 cm^{-1} silicon line.

2.4. Setup for fluorescence microscopy

In addition, a fluorescence photomicroscope (Olympus BX50) was used to confirm the presence of the fluorescent PS MPs in the analyzed cryosections of the mussels. The microscope is equipped with optical filters to visualize different wavelengths. In this work, 488 nm was used as excitation wavelength, and the fluorescent green line at 515 nm was detected. Origin 6.0 software was used for data analysis and plotting the spectra of the MPs. As it is technically almost impossible to find microparticles in large macroscopic areas in reasonable time by confocal Raman imaging (see below), full-field imaging with fluorescence microscopy was carried out beforehand, which allows us to easily identify suspicious particles and areas on which one can focus by Raman spectroscopy then.

3. Results and discussion

3.1. Microplastics in biological samples: Raman imaging

To advance sample preparation for optimized microscopy imaging regarding the identification of MPs, sections of 10 μm thickness were analyzed. In a first step, fluorescent PS MPs were detected by molecular fluorescence to ensure that MPs were inside the digestive system of the mussels. Then, the most promising areas of the cross-sections of the mussels were selected for further Raman analysis. Point-by-point Raman analyses were carried out in both the lumen and the epithelium of the stomach and gut.

The band of the aromatic carbon ring that appears at 1001 cm^{-1} was used to confirm the presence of PS in the sample (Fig. 1). The small size of the particles, together with the signal coming from the tissue of the mussels (sample matrix, see Fig. 1b), makes the detection of MPs challenging. In addition to PS MPs, other particles inside the digestive system were found, which turned the finding of MPs into a trial-and-error approach.

As can be seen, the number of PS MPs in the lumen (Fig. 1c) was higher than in the epithelium (Fig. 1a). In fact, aggregation of particles was noticed in the lumen. In the Raman spectra obtained from the PS MPs located in the epithelium, two strong and wide bands due to the matrix were always recorded at around 550 and 1100 cm^{-1}. However, in all cases, the features of PS MPs were visible (see the standard spectrum of fluorescent PS MPs in Fig. S1).

Once being certain that the MPs could be observed by point Raman analysis, Raman imaging was applied to detect the MPs in a more automatic and less trial-and-error manner. For that, a small section of the stomach was mapped using motorized stages with steps of 1 μm for both the X and Y axis. That way, a spectrum with 1 μm per pixel was obtained (see Fig. 2 as an example).

The scanned area is indicated by the rectangular region in Fig. 2 and corresponds to a surface of 387 μm × 151 μm. The time for mapping this area with steps of 1 μm × 1 μm was 64 h. In Fig. 2 we can see, in red, the PS MPs detected by Raman imaging after monitoring the intensity at 1001 cm^{-1} over the visible image of the mussel matrix. The color channels of the visible image in the figure have been modified for better contrast and visualization of the MPs.

As seen in Fig. 2, a high amount of PS MPs was accumulated in the lumen of the digestive tract, distributed all along the longitudinal mapped section of the stomach. This first Raman image was used to ascertain the ability of Raman to detect MPs automatically and to explore and fix the optimal parameters for further analysis in the epithelium in the same conditions. To the best of our knowledge, this is the first time that particles as small as 1 μm are detected in biological samples using Raman imaging. Although a section of the epithelium was mapped, no particles were observed in that specific area. Thus, the majority of the MPs observed in mussels were in the luminal cavity of digestive systems, which is in accordance with the observations by Calmão et al., 2023.

Cells with phagocytic activity, such as mussel hemocyte, can internalize MPs (Katsumiti et al., 2021; Von Moos et al., 2012). However, the capacity of MPs to cross very well-organized epitheliums, such as the digestive tract epithelium, and get incorporated into tissues, is not entirely proven. For the basic biological functions of any organism, it is essential to keep the luminal (outer) side, and the tissue (inner) side separated. Presently, the function of these barriers appeared to be properly maintained since the vast majority of

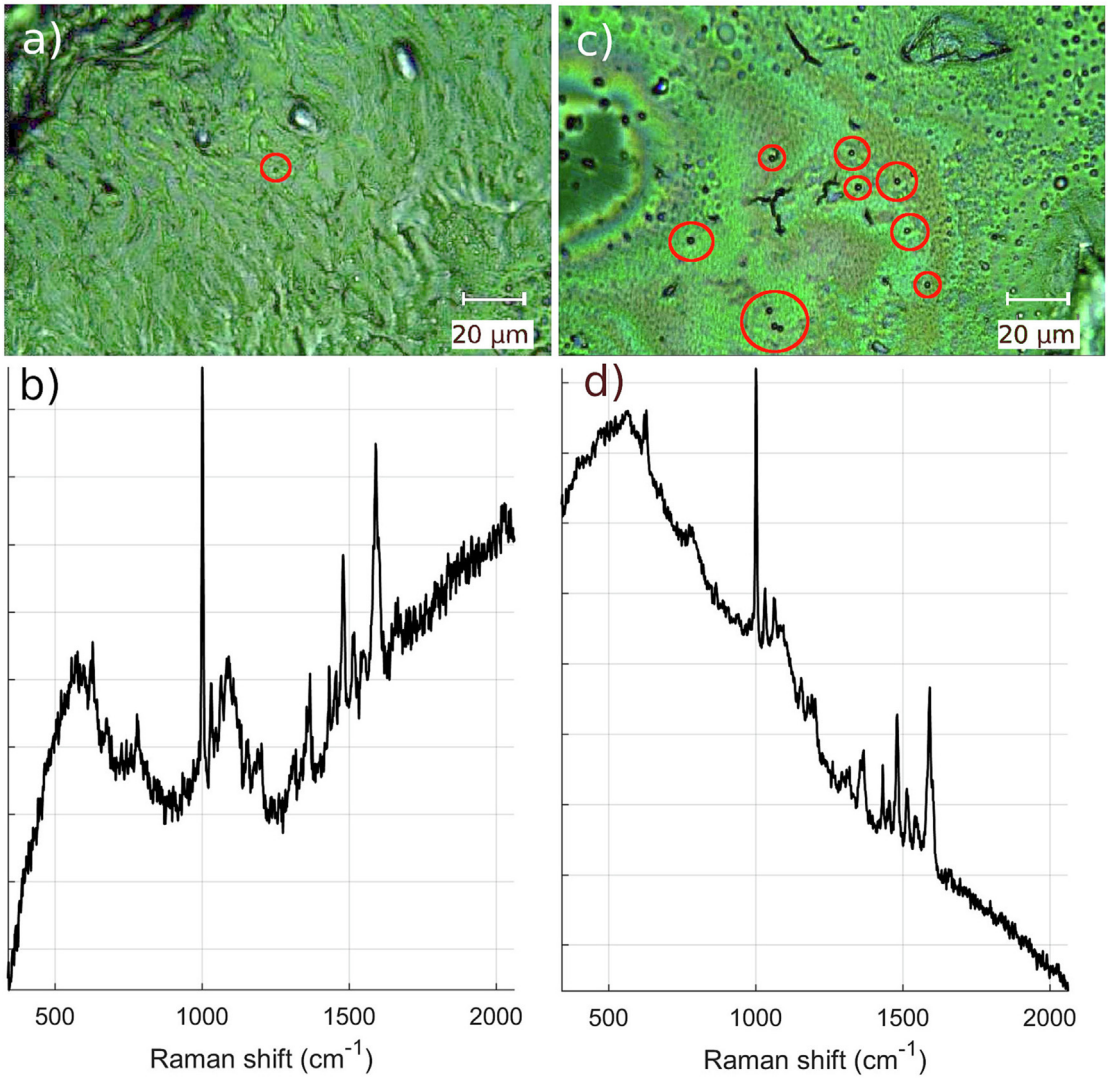

Fig. 1. Fluorescent polystyrene MPs in cryosections of *Mytilus galloprovincialis* marked with red circles. a) In gut epithelium at 50× magnification and corresponding Raman spectrum in b). c) In gut lumen at 50× magnification with corresponding Raman spectrum in d). (For interpretation of the references to color in this figure legend, the reader is referred to the web version of this article.)

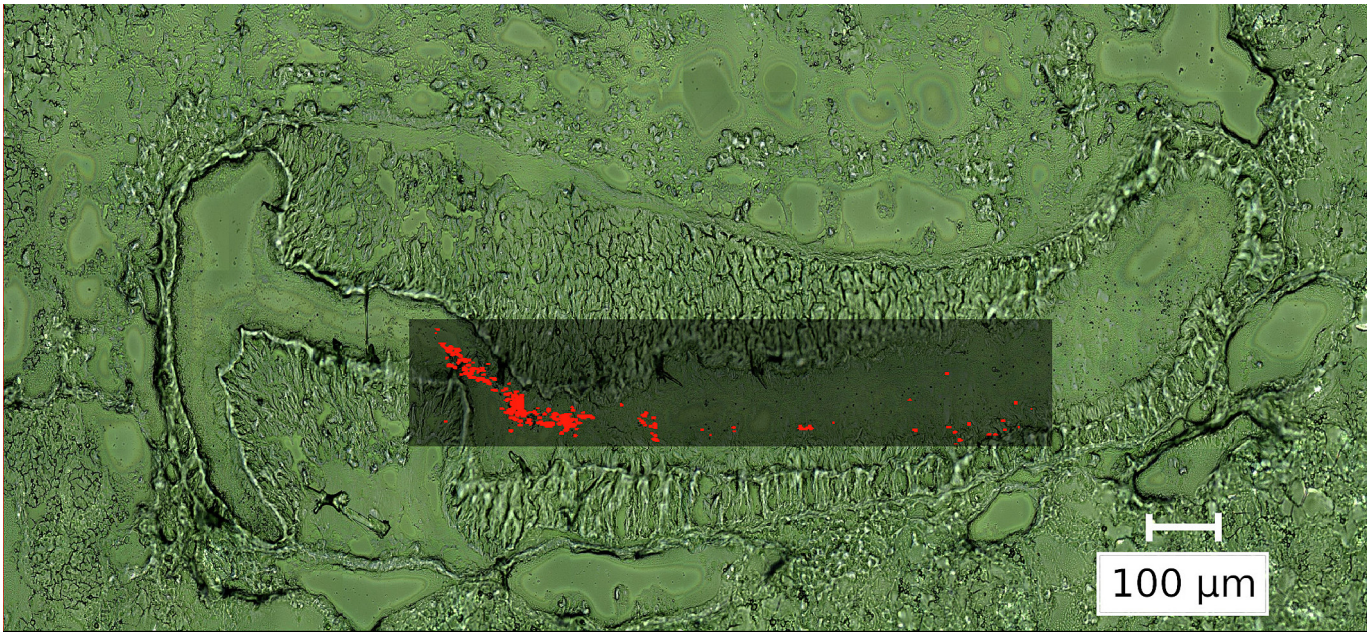

Fig. 2. Visible image (mosaic) of the analyzed stomach section obtained under a 50× objective of a DMLM Leica microscope coupled to the inVia Raman spectrometer. The mapped section of the stomach in which the fluorescent PS MPs of 1 μm were found is highlighted in the dark rectangle. The red points are the fluorescent PS MPs detected thanks to the intensity of its Raman band at 1001 cm^{-1}. (For interpretation of the references to color in this figure legend, the reader is referred to the web version of this article.)

MPs observed in the organisms were in the lumen and not internalized in epitheliums and cells. Damage of the cell membrane could condition the entrance of MPs into the epithelium. Nevertheless, little is known about the real membrane damage that would allow MPs to enter the epithelial cells or between them. Recently, apparent cell damage related to MPs was observed (Wang et al., 2021). However, under very different experimental settings with extremely high MP doses in cell culture. If the biological barriers were regularly surpassed by MPs or in animals under multiple environmental stress, the accumulation in tissues and transfer to higher level organisms in the trophic net would be exacerbated. To fully understand this problem, it is of utmost importance to develop powerful tools for the identification of plastics inside tissues. The approach used in the present study could illuminate real internalization into the cells and tissues of MPs and determine their real influence and direct damage.

To decide whether Raman imaging is useful for mapping and detecting particles inside the epithelium, first, the cryosections were observed under the fluorescence microscope (Fig. 3a, color channels of the image have been modified for better contrast and visualization). The cryosection with a higher content of MPs in that area was chosen to carry out a Raman mapping (Fig. 3b and c), whose scanning area is marked with a rectangle and corresponds to a surface of 21 μm × 38 μm. The time needed to map this area was 55 min with an integration time of 4 s, yielding a very good signal-to-noise ratio from the MPs. The Raman image (Fig. 3c) was generated following the same steps as the ones in Fig. 2. In Fig. 4, two typical Raman spectra are represented. The one in red color is the averaged spectrum of the area where PS MPs were found (showing the main Raman band at 1001 cm^{-1}), whereas the one in black is the averaged spectrum of the area where the mussel tissue was measured without MPs.

According to the results shown in Fig. 3, one might think that there are some PS MPs inside the epithelium of the gut; thus, our work represents one of the first studies in which the translocation of MPs to the tissue has been proved by Raman imaging after MPs uptake by mussels.

However, due to the ubiquitous occurrence of MPs nowadays, fortuitous contamination of the sample due to MPs deposition across the surface of the cryosection is a permanent threat, even under well-controlled laboratory conditions, as for example in clean rooms, laboratory and equipment cleaning, labware and lab clothes control. Moreover, even though the cryostat microtome uses a sharp blade to cut the tissue samples into thin slices, MPs might be moved by the blade (blade drag effect) from digestive lumens (eg. stomach, gut) to other tissues, a fact that would invalidate the proposed conclusions due to data misinterpretation. To our knowledge, this controversial issue has not been discussed in any previous work.

Microplastics in biological samples: Volumetric Raman chemical imaging (VRI).

To prove whether the particles were actually translocated from the lumen of the gut to the epithelium and internalized by epithelial cells, a full three-dimensional (3D) mapping (Volumetric Raman chemical imaging) from the gut epithelium was carried out. This map gives information about the composition, position, size and morphology of the sample, allowing us to know the location of the particles in all three spatial dimensions (X, Y and Z).

In Fig. 5, different adjacent cross-sectional planes of the epithelium are shown, separated by 1 μm depth. A total of 10 planes are shown. The number 0 corresponds to the surface of the cryosection, and the other planes are the ones underneath the surface of the cryosection. This map has a surface of 84 μm × 69 μm, multiplied by 10 planes, so that a total of 72 h were necessary to acquire the entire 3D spectral cuboid (1 μm × 1 μm × 1 μm motor step of the microscope stage). The Raman image was generated by the intensity of the characteristic Raman peak at 1001 cm^{-1} for PS MPs (in green color in Fig. 5) and by the intensity of the Raman band at 1008 cm^{-1}, characteristic of the matrix of the mussel (in red color in Fig. 5).

The image shows that the green dots only appeared in the first planes. From the plane located at −4 μm on the Z axis, the signal of the MPs disappeared, and only signals from the mussel matrix were observed. These observations demonstrate that the particles were not internalized by epithelial cells or between epithelial cells, since if they were, the particles would have appeared at different depths of the epithelium and would be surrounded by the epithelium. No MPs surrounded by tissue were found, which puts in doubt our initial results and conclusions regarding the actual presence of MPs in the epithelium.

Some authors support the hypothesis that the translocation of MPs to the epithelial cells could be done by phagocytosis, endocytosis, or another mechanism that allows the particles to pass through the intestinal barrier (Collard et al., 2017). During this process, a greater number of small MP particles can appear in the epithelium because the smaller particles are

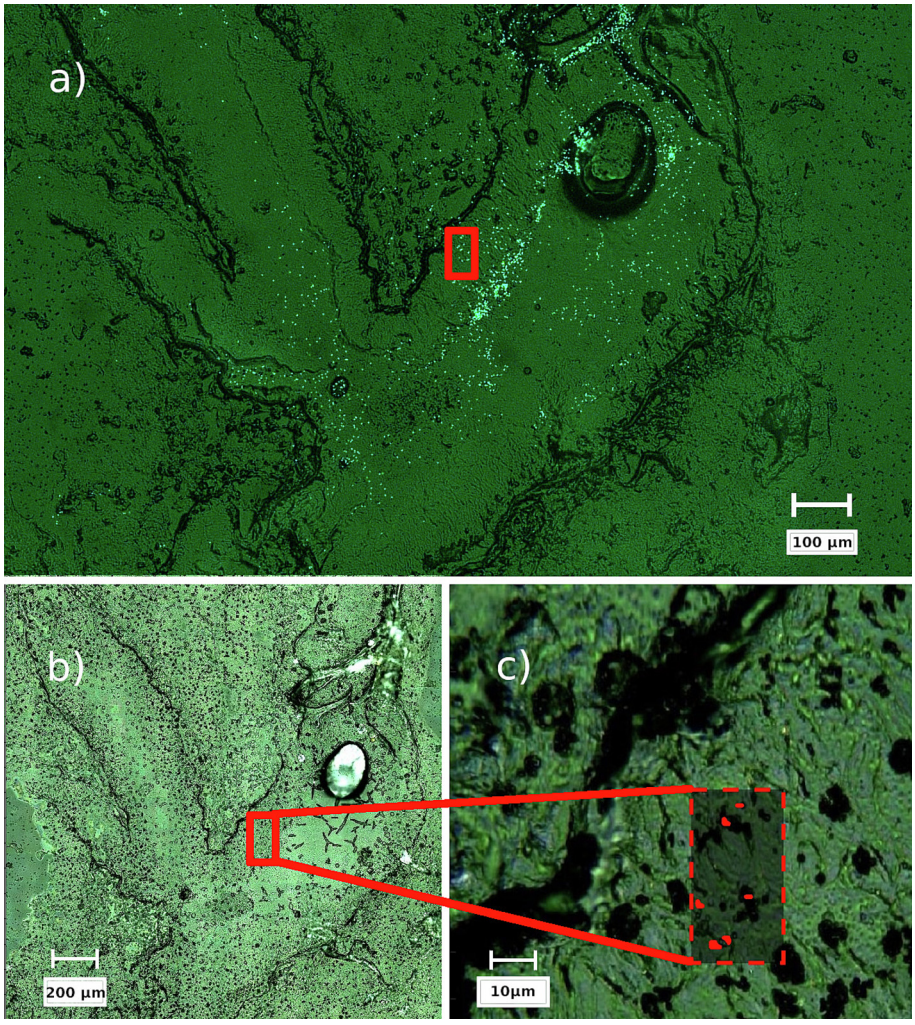

Fig. 3. a) Fluorescence microscopy image of PS MPs, showing in red the area with higher amount of PS microbeads in the gut epithelium. b) Visible image (mosaic) of the whole stomach section obtained under a 50× objective of a DMLM Leica microscope coupled to the inVia Raman spectrometer; in red the mapped area for Raman microscopy. c) Raman image of the mapped section of the epithelium in which the detected fluorescent PS microplastics of 1 µm are shown in red. (For interpretation of the references to color in this figure legend, the reader is referred to the web version of this article.)

more easily phagocytosed, possibly because the phagosomes within each cell can accommodate smaller particles (Browne et al., 2008).

However, as seen in our study, a surface imaging approach might not be enough to confirm the internalization of particles and avoid misinterpretation. Cryosectioning has been an established technique for many years, particularly applied for methods that do not support traditional histological techniques or when immediate results are required (Nguyen et al., 2019). Nevertheless, our present work reveals that even if the sample preparation seems correct, care must be taken when analyzing the results from Raman or any other high-resolution imaging technique to avoid misinterpretation.

In any case, some studies have highlighted the presence of plastic microparticles in the stomach epithelium (Browne et al., 2008). For example, Von Moos et al., 2012 determined the presence of MPs 0–80 µm in digestive epithelial cells, suggesting that particles were taken up via the mouth, transported to the gastrointestinal tract, and internalized into cells of the digestive system by endocytosis. González-Soto et al., 2019 observed individual 4.5 µm MPs within epithelial cells of the digestive tract, ducts, and digestive tubules. Collard et al., 2017 reported the presence of large (124 µm - 438 µm) MPs in the liver of the European anchovy. None of these works, as many others in the literature, discuss possible misinterpretation derived from the sample preparation and the cryotome/microtome blade drag effect on MPs, that is, MPs dragged from the lumens to the epithelium during sample preparation.

In Raman spectroscopy, the resolution for an image is constrained by the diffraction limit of the excitation laser spot (Fang et al., 2020). Due to the diffraction limit, the smallest lateral information volume is the Airy disc, which is a function of the numerical aperture and the excitation wavelength. Another limiting factor can be the pixel size of the camera/detector. Recently, Raman imaging was used to identify nanoplastics of 100 nm (Sobhani et al., 2020). Nevertheless, when mapped, the particles in the image showed a larger size of 300 nm – 400 nm, which is probably a result of the diffraction limit of the laser spot when focused on the nanoparticles for scanning and emitting the Raman signal (Fang et al., 2020). Under these considerations, it can be explained why in Fig. 5 the PS microparticles are represented much larger than their real size, when mapping their Raman signal. The diffraction limit is even more unfavorable when the particle size decreases, making analysis of very small particles almost impossible. Another possible explanation would be that the observed microparticles are not individual particles but aggregations of several ones.

4. Conclusions

Due to their small size and interference with organic and environmental material, separating and identifying microplastic particles in biological samples is challenging. However, we were able to efficiently characterize polystyrene microparticles down to a size of 1 µm in cryosections from

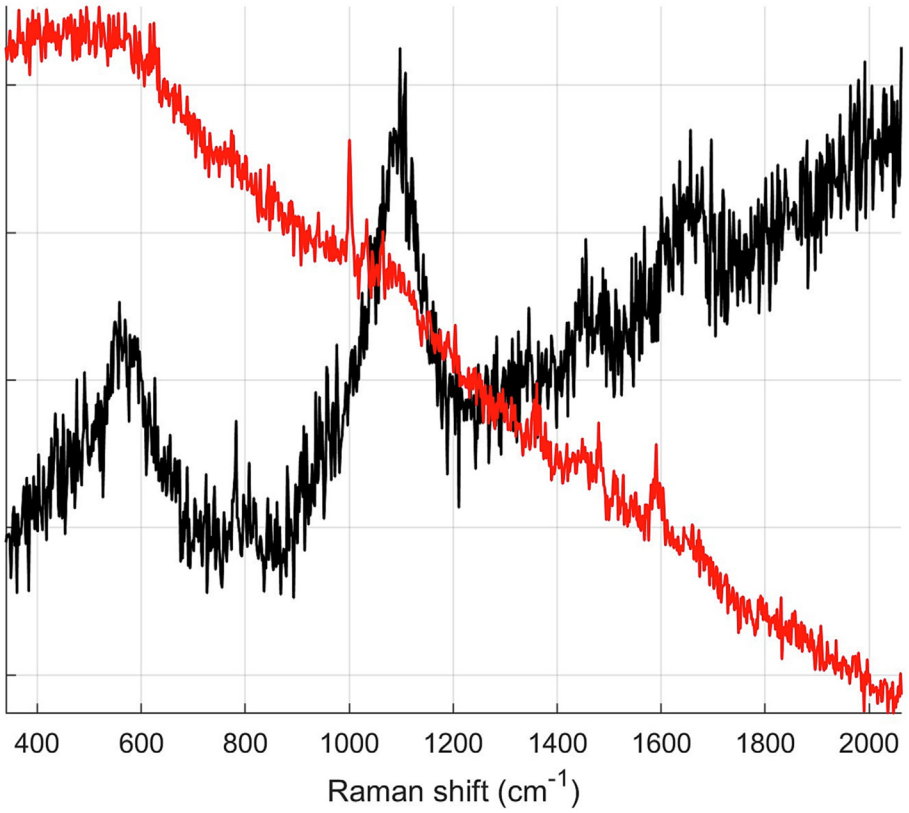

Fig. 4. Averaged Raman spectra of mussel tissue. Red: area on tissue with PS MPs with its characteristic peak at 1001 cm^{-1}; black: tissue without plastics. (For interpretation of the references to color in this figure legend, the reader is referred to the web version of this article.)

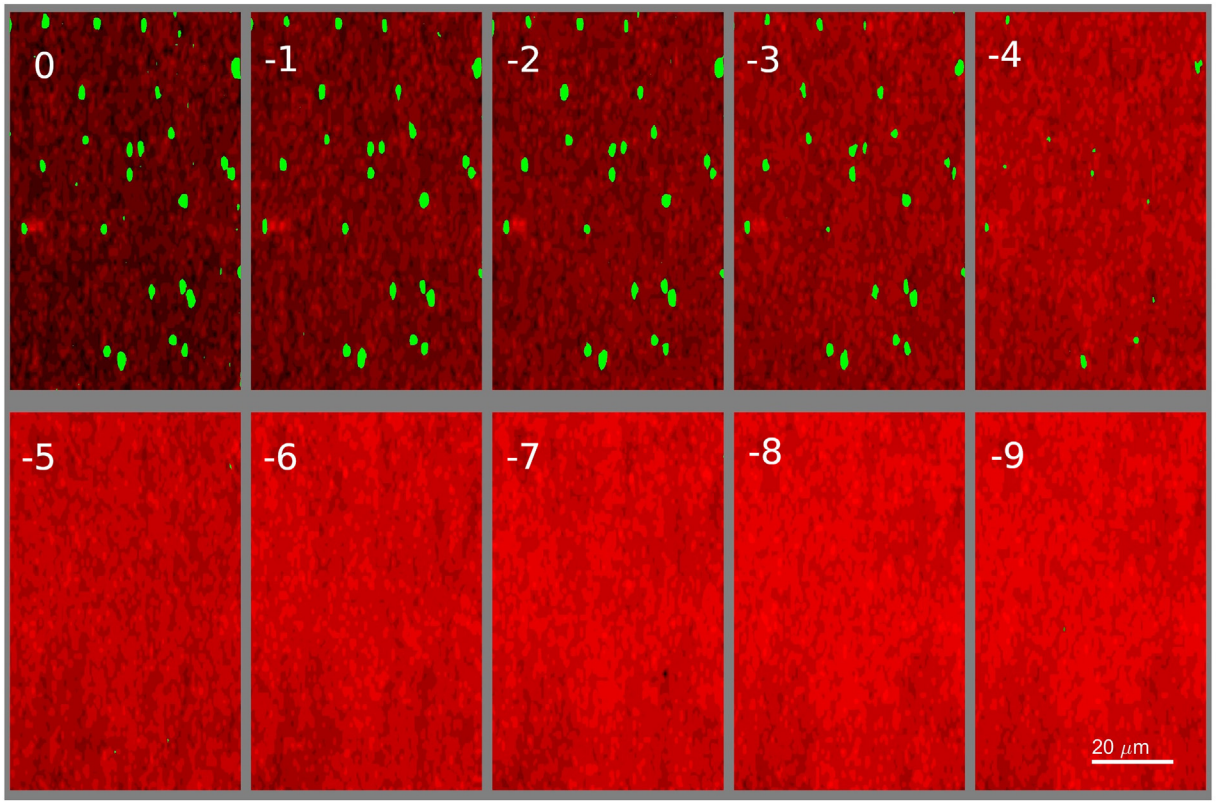

Fig. 5. Representation of the Z planes of the area of the gut epithelium mapped. Each image represents a different depth, with 1 μm difference in thickness between adjacent planes. Green color represents the fluorescent PS MPs, and the red color represents the mussel matrix. (For interpretation of the references to color in this figure legend, the reader is referred to the web version of this article.)

Mytilus galloprovincialis by Raman imaging. Sobhani et al., 2020 demonstrated that Raman mapping was useful to image and visualize an individual nanoplastic particle with a diameter of 100 nm, directly placed on a gold-coated microscope slide. Given that it has been demonstrated that MPs of 1 μm size can be identified in biological samples using Raman imaging, next important research steps have to focus on the detection and identification of nano and molecular plastics, which probably play a much stronger adverse role in biological systems.

Some particles of 1 μm size were observed in the gut epithelium, which could be one of the first detections of such small MPs in animal tissue. However, a further volumetric Raman chemical imaging analysis showed that the microplastics were located on the surface of the analyzed cryosection. We point out the microtome blade drag effect as a possible reason for the presence of microplastics on the surface of the analyzed epithelium. Even though cryosection is still a highly useful preparation technique that allows for visualization of particles directly on mussel tissue where they are naturally accumulated, and gives more biologically relevant information than other more commonly used methods, as for example chemical digestion, precautions have to be taken for a conclusive data interpretation.

In literature, research can be found that shows microplastic presence in several tissues by analyzing them with analytical techniques similar to those used in the present work. It is not our intention to put such results in doubt, but the present work points out the necessity of appropriate data interpretation and the need to go a step further than just surface imaging analysis. As a result, it turns out that volumetric Raman imaging analysis is an important and essential analytical technique to analyze the distribution of particles and confirm their presence at tissue and cellular levels; otherwise, false positive detections and wrong conclusions could easily be drawn.

Based on our analytical findings, we conclude that surface mapping is insufficient for characterizing and locating microplastics in and on tissue slices, as volumetric Raman imaging analysis shows that the microparticles did not translocate into epithelial cells, at least, not in our analyzed samples. In other words, surface mapping is sufficient for identifying MPs, but gives limited information about the real 3D location in or on tissue.

Supplementary data to this article can be found online at https://doi.org/10.1016/j.scitotenv.2023.162810.

CRediT authorship contribution statement

Alba Benito-Kaesbach: Paper writing, Raman imaging measurements.

Jose Manuel Amigo: Data treatment (imaging), Figure editing.

Urtzi Izagirre: Paper writing, Sampling of the mussels and all experiments related with the mussels feeding with microplastics.

Nerea Garcia-Velasco: Sampling of the mussels and all experiments related with the mussels feeding with microplastics.

Laura Arévalo: Data treatment (imaging).

Andreas Seifert: Paper writing and correcting, coordinator of the experiments and staff.

Kepa Castro: Paper writing, Raman imaging measurements, Figure editing.

Data availability

Data will be made available on request.

Declaration of competing interest

The authors declare the following financial interests/personal relationships which may be considered as potential competing interests: Kepa Castro reports financial support was provided by Basque Business Development Agency. Andreas Seifert reports financial support was provided by Ministry of Science Technology and Innovations. Andreas Seifert reports financial support was provided by Basque Business Development Agency. Urtzi Izagirre reports financial support was provided by Ministry of Economic Affairs and Digital Transformation. Urtzi Izagirre reports financial support was provided by Basque Business Development Agency.

Acknowledgements

This work was funded by Basque Government (KK 2021/00001 ELKARTEK 2021/2022, IT1743-22); MINECO (PID 2020-118685RB-I00, PLASTeMER); further financial support by grant CEX2020-001038-M funded by MCIN/AEI/ 10.13039/501100011033.

References

Araujo, C.F., Nolasco, M.M., Ribeiro, A.M., Ribeiro-Claro, P.J., 2018. Identification of microplastics using Raman spectroscopy: latest developments and future prospects. Water Res. 142, 426–440.

Browne, M.A., Dissanayake, A., Galloway, T.S., Lowe, D.M., Thompson, R.C., 2008. Ingested microscopic plastic translocates to the circulatory system of the mussel, Mytilus edulis (L.). Environ. Sci. Technol. 42, 5026–5031.

Calmão, M., Blasco, N., Benito, A., Thoppil, R., Torre-Fernandez, I., Castro, K., Izagirre, U., Garcia-Velasco, N., Soto, M., 2023. Time-course distribution of fluorescent microplastics in target tissues of mussels and polychaetes. Chemosphere 311, 137087.

Chen, X., Zhang, C., Lin, P., Huang, K.C., Liang, J., Tian, J., Cheng, J.X., 2017. Volumetric chemical imaging by stimulated raman projection microscopy and tomography. Nat. Commun. 8, 15117.

Collard, F., Gilbert, B., Compère, P., Eppe, G., Das, K., Jauniaux, T., Parmentier, E., 2017. Microplastics in livers of European anchovies (Engraulis encrasicolus, L.). Environ. Pollut. 229, 1000–1005.

Dehaut, A., Cassone, A.L., Frère, L., Hermabessiere, L., Himber, C., Rinnert, E., Rivière, G., Lambert, C., Soudant, Ph., Huvet, A., Duflos, G., Paul-Pont, I., 2016. Microplastics in seafood: benchmark protocol for their extraction and characterization. Environ. Pollut. 215, 223–233.

De-la-Torre, G.E., Dioses-Salinas, D.C., Pizarro-Ortega, C.I., Saldaña-Serrano, M., 2020. Global distribution of two polystyrene-derived contaminants in the marine environment: a review. Mar. Pollut. Bull. 161, 111729.

Elert, A.M., Becker, R., Duemichen, E., Eisentraut, P., Falkenhagen, J., Sturm, H., Braun, U., 2017. Comparison of different methods for MP detection: what can we learn from them, and why asking the right question before measurements matters? Environ. Pollut. 231, 1256–1264.

Enders, K., Lenz, R., Stedmon, C.A., Nielsen, T.G., 2015. Abundance, size and polymer composition of marine microplastics ≥ 10 μm in the Atlantic Ocean and their modelled vertical distribution. Mar. Pollut. Bull. 100, 70–81.

Erni-Cassola, G., Gibson, M.I., Thompson, R.C., Christie-Oleza, J.A., 2017. Lost, but found with Nile red: a novel method for detecting and quantifying small microplastics (1 mm to 20 μm) in environmental samples. Environ. Sci. Technol. 51, 13641–13648.

Fang, C., Sobhani, Z., Zhang, X., Gibson, C.T., Tang, Y., Naidu, R., 2020. Identification and visualisation of microplastics/nanoplastics by raman imaging (ii): smaller than the diffraction limit of laser? Water Res. 183, 116046.

González-Soto, N., Hatfield, J., Katsumiti, A., Duroudier, N., Lacave, J.M., Bilbao, E., Orbea, A., Navarro, E., Cajaraville, M.P., 2019. Impacts of dietary exposure to different sized polystyrene microplastics alone and with sorbed benzo[a]pyrene on biomarkers and whole organism responses in mussels Mytilus galloprovincialis. Sci. Total Environ. 684, 548–566.

Imhof, H.K., Laforsch, C., Wiesheu, A.C., Schmid, J., Anger, P.M., Niessner, R., Ivleva, N.P., 2016. Pigments and plastic in limnetic ecosystems: a qualitative and quantitative study on microparticles of different size classes. Water Res. 98, 64–74.

Irazola, M., Garmendia, L., Zaldibar, B., Izagirre, U., Bilbao, E., Danielsson, S., Bignert, A., Castro, K., Etxebarria, N., Soto, M., Marigomez, I., 2015. Combination of microscopic and spectroscopic techniques to study the presence and the effects of microplastics in mussels. Proceedings of the MOL2NET, Sciforum Electronic Conference Series https://doi.org/10.3390/MOL2NET-1-c010.

Jin-Feng, D.I.N.G., Jing-Xi, L.I., Cheng-Jun, S.U.N., Chang-Fei, H.E., Jiang, F.H., Feng-Lei, G.A.O., Zheng, L., 2018. Separation and identification of microplastics in digestive system of bivalves. Chin. J. Anal. Chem. 46, 690–697.

Kallepitis, C., Bergholt, M.S., Mazo, M.M., Leonardo, V., Skaalure, S.C., Maynard, S.A., Stevens, M.M., 2017. Quantitative volumetric Raman imaging of three dimensional cell cultures. Nat. Commun. 8, 14843.

Käppler, A., Fischer, D., Oberbeckmann, S., Schernewski, G., Labrenz, M., Eichhorn, K.J., Voit, B., 2016. Analysis of environmental microplastics by vibrational microspectroscopy: FTIR, Raman or both? Anal. Bioanal. Chem. 408, 8377–8391.

Katsumiti, A., Losada-Carrillo, M.P., Barros, M., Cajaraville, M.P., 2021. Polystyrene nanoplastics and microplastics can act as trojan horse carriers of benzo(a)pyrene to mussel hemocytes in vitro. Sci. Rep. 11, 22396.

Kolandhasamy, P., Su, L., Li, J., Qu, X., Jabeen, K., Shi, H., 2018. Adherence of microplastics to soft tissue of mussels: a novel way to uptake microplastics beyond ingestion. Sci. Total Environ. 610, 635–640.

Lenz, R., Enders, K., Stedmon, C.A., Mackenzie, D.M., Nielsen, T.G., 2015. A critical assessment of visual identification of marine microplastic using Raman spectroscopy for analysis improvement. Mar. Pollut. Bull. 100, 82–91.

Lenz, R., Enders, K., Nielsen, T.G., 2016. Microplastic exposure studies should be environmentally realistic. PNAS 113, E4121–E4122.

Leung, M.M.L., Ho, Y.W., Lee, C.H., Wang, Y., Hu, M., Kwok, K.W.H., Chua, S.L., Fang, J.K.H., 2021. Improved Raman spectroscopy-based approach to assess microplastics in seafood. Environ. Pollut. 117648.

Levermore, J.M., Smith, T.E., Kelly, F.J., Wright, S.L., 2020. Detection of microplastics in ambient particulate matter using raman spectral imaging and chemometric analysis. Anal. Chem. 92, 8732–8740.

Li, J., Lusher, A.L., Rotchell, J.M., Deudero, S., Turra, A., Bråte, I.L.N., Sun, C., Hossain, M.S., Li, Q., Kolandhasamy, P., Shi, H., 2019. Using mussel as a global bioindicator of coastal microplastic pollution. Environ. Pollut. 244, 522–533.

Lin, P., Ni, H., Li, H., Vickers, N.A., Tan, Y., Gong, R., Bifano, T., Cheng, J.X., 2020. Volumetric chemical imaging in vivo by a remote-focusing stimulated Raman scattering microscope. Opt. Express 28, 30210–30221.

Mattson, E.C., Aboualizadeh, E., Barabas, M.E., Stucky, C.L., Hirschmugl, C.J., 2013. Opportunities for live cell FT-infrared imaging: macromolecule identification with 2D and 3D localization. Int. J. Mol. Sci. 14, 22753–22781.

Mendoza, L.M.R., Karapanagioti, H., Álvarez, N.R., 2018. Micro (nanoplastics) in the marine environment: current knowledge and gaps. Curr. Opin. Environ. Sci. Health 1, 47–51.

Nguyen, B., Claveau-Mallet, D., Hernandez, L.M., Xu, E.G., Farner, J.M., Tufenkji, N., 2019. Separation and analysis of microplastics and nanoplastics in complex environmental samples. Accounts Chem. Res. 52, 858–866.

Noventa, S., Boyles, M.S.P., Seifert, A., Belluco, S., Jiménez, A.S., Johnston, H.J., Tran, L., Fernandes, T.F., Orsini, M., Corami, F., Castro, K., Mutinelli, F., Boldrin, M., Puntes, V., Sotoudeh, M., Mascarello, G., Tiozzo, B., McLean, P., Ronchi, F., Booth, A.M., Koelmans, A.A., Losasso, C., Mughini-Gras, L., 2021. Paradigms to assess the human health risks of nano- and microplastics. Microplastics and Nanoplastics 1 (9).

Primpke, S., Godejohann, M., Gerdts, G., 2020. Rapid identification and quantification of microplastics in the environment by quantum cascade laser-based hyperspectral infrared chemical imaging. Environ. Sci. Technol. 54, 15893–15903.

Shim, W.J., Hong, S.H., Eo, S.E., 2017. Identification methods in microplastic analysis: a review. Anal. Methods 9, 1384–1391.

Sobhani, Z., Zhang, X., Gibson, C., Naidu, R., Megharaj, M., Fang, C., 2020. Identification and visualisation of microplastics/nanoplastics by Raman imaging (i): down to 100 nm. Water Res. 174, 115658.

Soto, M., Kortabitarte, M., Marigómez, I., 1995. Bioavailable heavy metals in estuarine waters as assessed by metal/shell-weight indices in sentinel mussels Mytilus galloprovincialis. Mar. Ecol. Prog. Ser. 125, 127–136.

Tarafdar, A., Choi, S.H., Kwon, J.H., 2022. Differential staining lowers the false positive detection in a novel volumetric measurement technique of microplastics. J. Hazard. Mater. 432, 128755.

Vianello, A., Boldrin, A., Guerriero, P., Moschino, V., Rella, R., Sturaro, A., Da Ros, L., 2013. Microplastic particles in sediments of lagoon of Venice, Italy: first observations on occurrence, spatial patterns and identification. Estuar. Coast. Shelf Sci. 130, 54–61.

Von Moos, N., Burkhardt-Holm, P., Köhler, A., 2012. Uptake and effects of microplastics on cells and tissue of the blue mussel Mytilus edulis L. After an experimental exposure. Environ. Sci. Technol. 46, 11327–11335.

Wang, S., Hu, M., Zheng, J., Huang, W., Shang, Y., Fang, J.K.H., Shi, H., Wang, Y., 2021. Ingestion of nano/micro plastic particles by the mussel Mytilus coruscus is size dependent. Chemosphere 263, 127957.

Wei, M., Shi, L., Shen, Y., Zhao, Z., Guzman, A., Kaufman, L.J., Wei, L., Min, W., 2019. Volumetric chemical imaging by clearing-enhanced stimulated raman scattering microscopy. PNAS 116, 6608–6617.

Wright, S.L., Thompson, R.C., Galloway, T.S., 2013. The physical impacts of microplastics on marine organisms: a review. Environ. Pollut. 178, 483–492.

Xu, J.L., Thomas, K.V., Luo, Z., Gowen, A.A., 2019. FTIR and Raman imaging for microplastics analysis: state of the art, challenges and prospects. TrAC Trends Anal. Chem. 119, 115629.

Yu, J., Wang, P., Ni, F., Cizdziel, J., Wu, D., Zhao, Q., Zhou, Y.Mar, 2019. Characterization of microplastics in environment by thermal gravimetric analysis coupled with Fourier transform infrared spectroscopy. Pollut. Bull. 145, 153–160.

Zhu, J., Wang, C., 2020. Recent advances in the analysis methodologies for microplastics in aquatic organisms: current knowledge and research challenges. Anal. Methods 12, 2944–2957.